



## Study geometrical, electronic and spectroscopic properties of BeO wurtzoids via DFT

K. Ahmed Sameer, T. Mohammed Hussein \*

Department of Physics, College of Science, University of Baghdad, Baghdad, Iraq

### ARTICLE INFO

#### Article history:

Available online 15 February 2021

#### Keywords:

BeO Wurtzoid  
Electronic properties  
DFT

### ABSTRACT

The electronic and spectroscopic properties of BeO wurtzoids structure were investigated by using ab-initio density functional theory and generalized gradient approximation calculations combined with many-body. All calculations were carried out using Gaussian 09 program. Electronic properties including energy gap, density of state and bond length, as well as Spectroscopic properties of infrared and Raman scattering, force constant, reduced mass and longitudinal optical patterns. The geometrical structure of BeO molecules and wurtzoids nanostructure were studied with the help using Gauss view 05 program. The energy gap of Wurtzoid, wurtzoid2c and triwurtzoid was found to be (6.813, 7.13499 and 7.02669 eV) respectively. Those values agreed with theoretical values for BeO wurtzite (8.57 eV), and compare with the experimental value of BeO bulk (10.6 eV). The Spectroscopic study of IR and Raman scattering, force constant, and reduced mass and longitudinal optical modes as a function of frequencies are agreed with the experimental results.

© 2021 Elsevier Ltd. All rights reserved.

Selection and peer-review under responsibility of the scientific committee of the 3rd International Conference on Materials Engineering & Science.

## 1. Introduction

Beryllium oxide (BeO) is a white inorganic mineral that can be grown in the laboratory and crystallizes in the form of hexagonal wurtzite, but can also be contained at elevated temperatures in the cubic zincblend structure. The hexagonal structure is more stable by approximately (5.6) meV per pair of atoms than the cubic structure, according to theoretical calculations [1]. Continenza et al. [2], BeO has excellent physicochemical properties, such as high band gap energy (10.6 eV) [3], melting point ( $2532 \pm 10$  °C) [4], electrical resistivity ( $>10^{14}$   $\Omega$ .cm) [5], and dielectric constant (6.9) [6]. BeO has high thermal conductivity (330 W/K.m), among the well-known oxide materials (SiO<sub>2</sub>, Al<sub>2</sub>O<sub>3</sub>, HfO<sub>2</sub>, ZrO<sub>2</sub>), BeO has the highest thermal conductivity [7]. The properties of BeO make it the best practical candidate as a dielectric material gate in SiC-based metal-oxide semiconductor field-effect-transistors (MOSFETs). Based on Gibbs free configuration energy, BeO is the most thermally stable dielectric. The high thermal conductivity indicates less soft phonon modes compared to other high k dielec-

trics, according to the size, similarity between the Be and O atoms [8,9]. Soft phonon modes in gate dielectrics interference with the movement of channel carriers, degrading the carrier mobility in Si and III-V metal oxide semiconductor field-effect transistors (MOSFETs). Thus, a small number of soft phonons is preferred in high-k gate dielectrics [10]. Therefore, BeO film as a gate insulator, high channel mobility can be obtained, and at the same time, self-heating problems can be alleviated. BeO is also a mechanically strong material that can be used in transparent telescope mirror coatings, because of its electromagnetic spectrum sensitivity and radiation tolerance in the Schumann region. BeO can be used to monitor global events from lightning activity and earthquake prediction to changes in atmospheric water vapor that can affect global temperatures for elect And applications in outer space [11]. Several researchers have worked on the theoretical analysis of structural, electronic and optical properties for different molecules to form nano-scale limited wurtziod molecules that emerge in the hexagonal structures ( $a = b \neq c$ ) of material and have the same of its properties by using simulation by programs Gaussian 09 and inverse the diamondoids that came from the cubic structure ( $a = b = c$ ) of material in bulk of solid materials [12–19].

In this study, geometrical, electronic and spectroscopic characteristics of the molecular and nanostructures of BeO as nanotubes

\* Corresponding author.

E-mail address: [ahmed.sameer1204@sc.uobaghdad.edu.iq](mailto:ahmed.sameer1204@sc.uobaghdad.edu.iq) (T. Mohammed Hussein).

has investigated using Ab-initio approximation method that depends on Density Functional Theory (DFT) method.

## 2. Theory

This paper employs one of the theoretical approximations methods to simulate the features and nanostructures of BeO nanotubes includes all electrons in the molecules at generalized gradient approximation (GGA) and Density Functional Theory (DFT) which is a powerful tool for ground-state properties, but not for excited states. Also, due to an unjustified interpretation of the Kohn–Sham (KS) eigenvalues as single-particle excitation energies it [20]. By using B3LYP (Becke, three-parameters, Lee-Yang-Parr) as basis set with 6-31G\*, it sometimes written 6-31G(d) [21]. These calculations have been performed by Gaussian 09 program [22]. The spectroscopic properties calculations have been completed by using 0.960 as a scale factor to give the corrections on the frequencies, this scale associated with 6-31G\* [21].

In this study, the molecular- nanoscale limited of BeO is investigated. In the beginning, the BeO of wurtzite form can be used as seeds for the present molecules.

Fig. 1 shows the structures wurtziods include the wurtziod  $\text{Be}_7\text{O}_7$  (one nanotube), wurtziod2c  $\text{Be}_{13}\text{O}_{13}$  (two nanotubes along c-lattice constant), and triwurtziod  $\text{Be}_{21}\text{O}_{21}$  (three nanotubes) at nanoscale size.

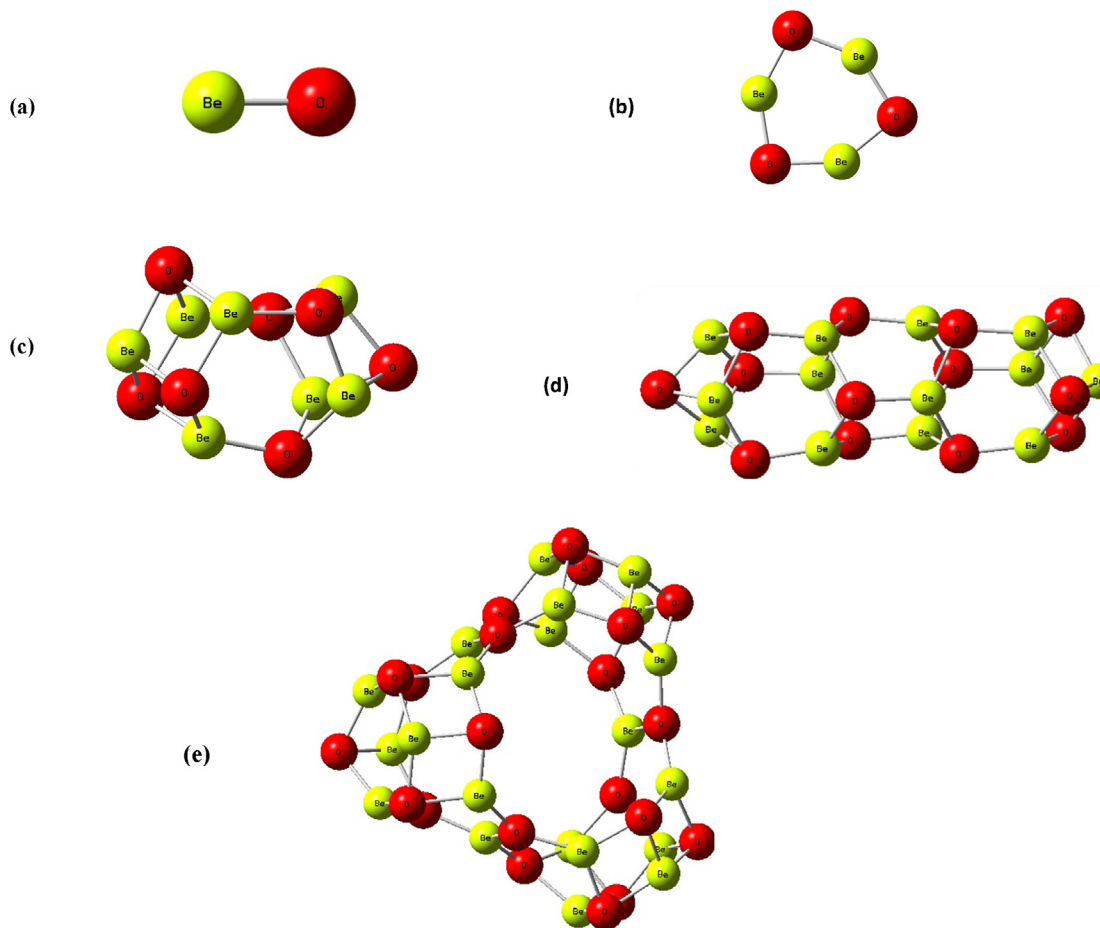


Fig. 1. (a) BeO molecule, (b) cyclohexane  $\text{Be}_3\text{O}_3$ , (c) wurtzoid  $\text{Be}_7\text{O}_7$ , (d) wurtzoid2c  $\text{Be}_{13}\text{O}_{13}$ , (e) triwurtzoid  $\text{Be}_{21}\text{O}_{21}$ , after geometrical optimization structure.

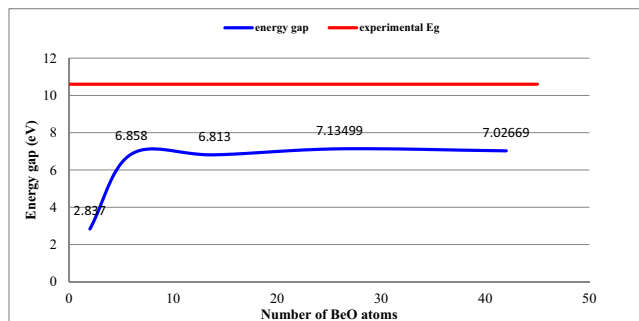


Fig. 2. The energy gap as a function of number of atoms for BeO molecule, cyclohexane  $\text{Be}_3\text{O}_3$ , wurtzoid  $\text{Be}_7\text{O}_7$ , wurtzoid2c  $\text{Be}_{13}\text{O}_{13}$  and triwurtzoid  $\text{Be}_{21}\text{O}_{21}$ .

## 3. Results and discussion

### 3.1. Electronic properties

#### 3.1.1. Energy gap

The energy gap is one of the most important electronic properties of solids. The energy gap generally refers to the energy difference between the top of the valence band, which is called the highest occupied molecular orbital (HOMO), and the bottom of

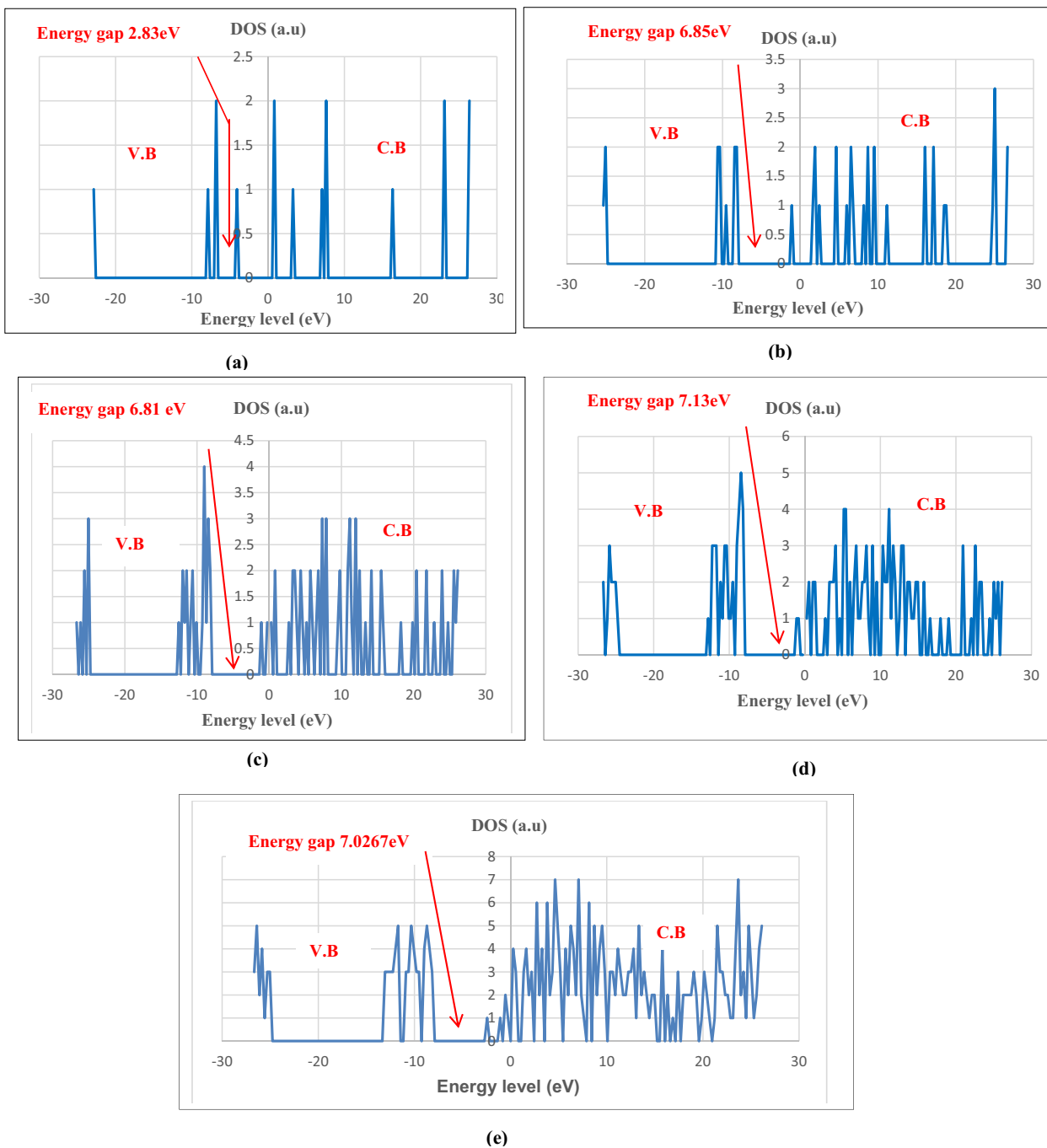


**Fig. 3.** (a) The density of states as a function of energy levels for BeO molecule, (b) The density of states as a function of energy levels for Cyclohexane Be<sub>3</sub>O<sub>3</sub>, (c) The density of states as a function of energy levels for wurtzoid Be<sub>7</sub>O<sub>7</sub>, (d) The density of states as a function of energy levels for wurtzoid2C Be<sub>13</sub>O<sub>13</sub>, (e) The density of states as a function of energy levels for triwurtzoid Be<sub>21</sub>O<sub>21</sub>, and show the energy gap for every one.

the conduction band, which is called the lowest unoccupied molecular orbital (LUMO). It is found in insulators and semiconductors [23]. The LUMO levels are more sensitive than HOMO levels for surface effects, through small difference between two levels especially when the collections be large. Fig. 2 shows the energy gap in (eV) as a function of number of atoms of BeO and compare with the theoretical and experimental values of bulk.

We notice that the energy gap increases with the number of atoms, because of the existence of dangling bonds on the surface of BeO. The energy gap is lower than the experimental value. Those dangling bonds levels are inside the energy gap. As we increase the size of BeO molecule the effect of the surface dangling bonds vanishes and the energy gap approaches the experimental value. The energy gap of wurtzoid, wurtzoid2c and triwurtzoid is (6.813,

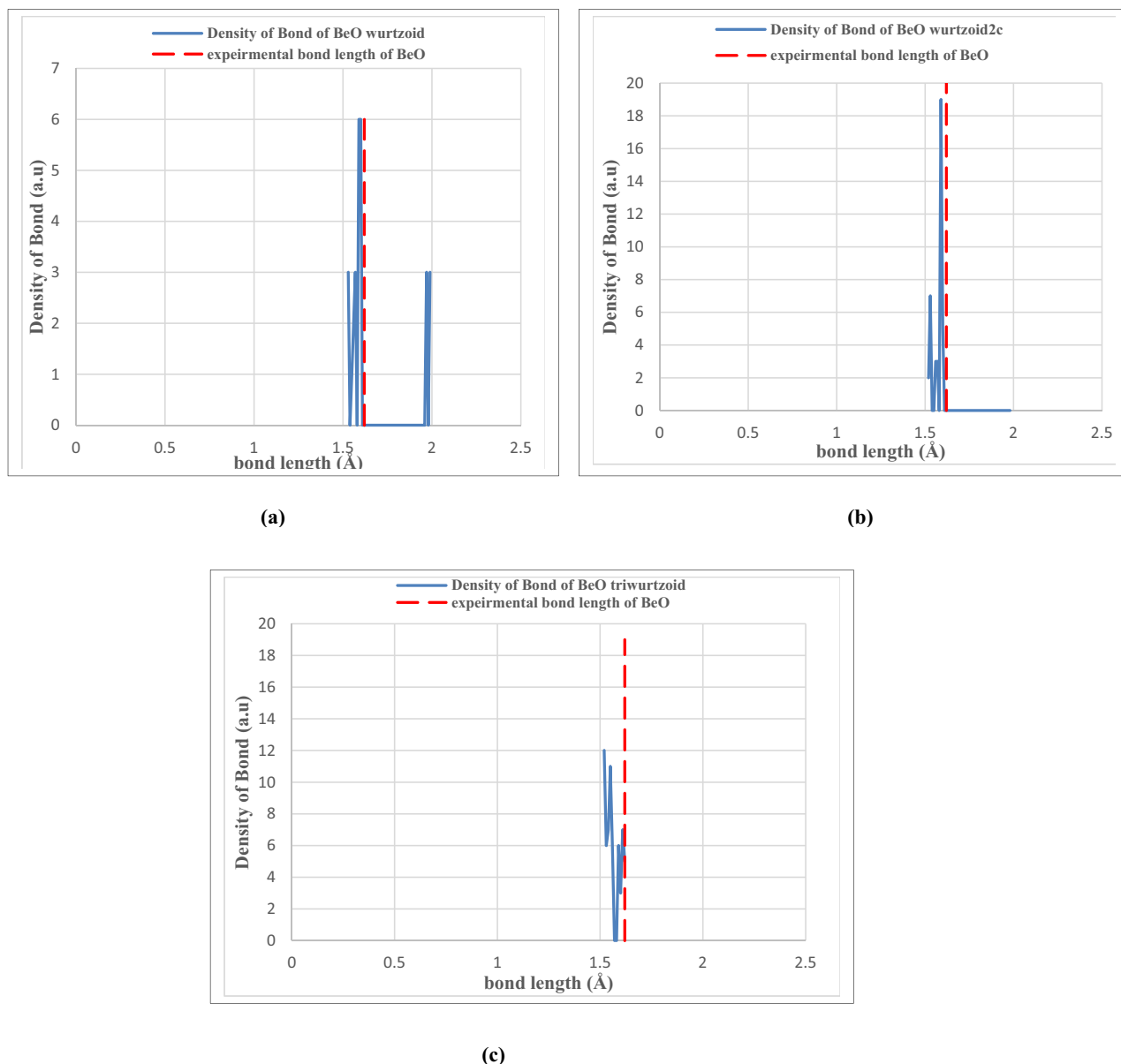


**Fig. 4.** (a) The density of bond of BeO wurtzoid, (b) The density of bond of BeO wurtzoid2c, (c) The density of bond of BeO triwurtzoid, compare with experimental Be- O Bond lengths.

7.13499 and 7.02669 eV) respectively, agrees with the theoretical values of BeO wurtzite (8.57 eV) [24] and approximated to the experimental value of BeO bulk (10.6 eV) [3]. Therefore it can be considered a good results.

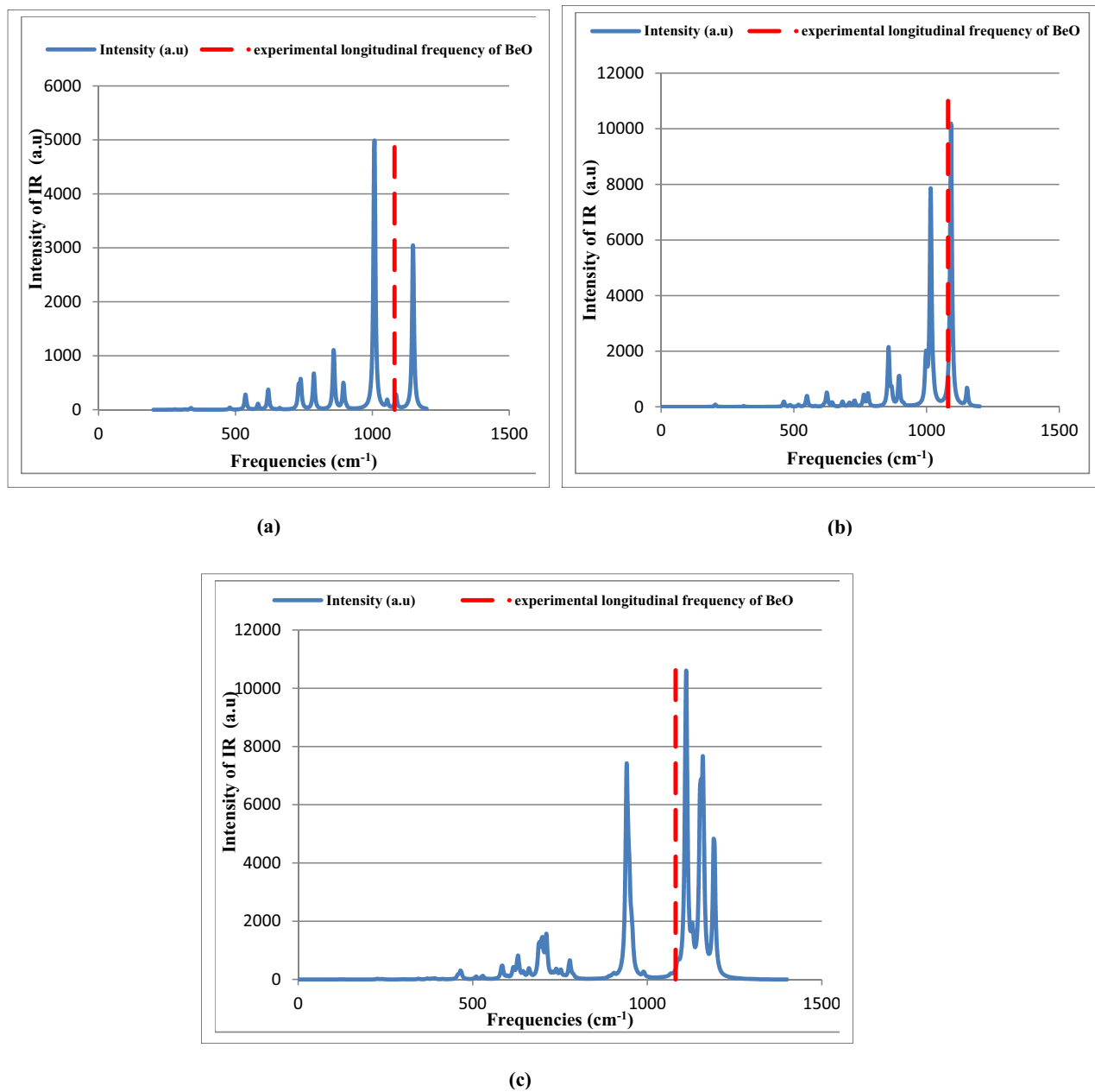
### 3.1.2. Density of states:

Fig. 3(a,b,c,d and e) shows the densities of states of BeO molecule, Cyclohexane  $\text{Be}_3\text{O}_3$ , wurtziod  $\text{Be}_7\text{O}_7$ , wurtzoid2c  $\text{Be}_{13}\text{O}_{13}$  and triwurtzoid  $\text{Be}_{21}\text{O}_{21}$  respectively, as a functions to energies levels, the edges of the conduction and valence bands are generally less degenerate than the states at the middle of these bands.

We can see that the energy gap is small for small BeO molecules, because of the large surface to volume ratio. As we increase the size of the molecules of the surface to volume ratio decrease and energy gap increase.

### 3.1.3. Density of bond length

Fig. 4(a,b and c) shows the distribution of bond length of BeO wurtzoid, BeO wurtzoid2c and BeO triwurtzoid, respectively and compare with experimental values of bond length of BeO bulk. It found that the values of bond length of Be-O wurtzoid, wurtzoid2c and triwurtzoid are (1.61, 1.59 and 1.52 Å) respectively. Those results were agreed with theoretical values (1.57 Å) [25], (1.52,



**Fig. 5.** (a) The intensity of IR of wurtzoid Be<sub>7</sub>O<sub>7</sub>, (b) The intensity of IR of wurtzoid2c Be<sub>13</sub>O<sub>13</sub>, (c) The intensity of IR of triwurtzoid Be<sub>21</sub>O<sub>21</sub>, compare with the experimental longitudinal frequency of BeO bulk.

1.58 Å) [26], and experimental value (1.62 Å) [27], so it can be considered as reasonable results.

### 3.2. Spectroscopy properties

#### 3.2.1. IR and Raman spectra

Fig. 5(a, b and c) shows the intensity of IR of BeO wurtzoid, wurtzoid2c and triwurtzoid respectively, as a function of frequencies. The results were compared with the experimental value of longitudinal frequency (LO) of BeO bulk. From this figure, two

regions (1006 and 1150) cm<sup>-1</sup> are observed and the maximum intensity is 4972 a.u at 1006 cm<sup>-1</sup> for wurtzoid, while for wurtzoid2c (1015 and 1092) cm<sup>-1</sup> and the maximum intensity is 10,181 a.u at 1092 cm<sup>-1</sup>, but four regions (940, 1111, 1159 and 1190) cm<sup>-1</sup> are found in triwurtzoid and the maximum intensity is 10,593 a.u at 1111 cm<sup>-1</sup>. we can observe from Fig. 6(a,b and c) that these regions are very low intensity in Raman spectra. The maximum intensity of Raman is (1.32 a.u at 894 cm<sup>-1</sup> for wurtzoid, 1.87 a.u at 856 cm<sup>-1</sup> for wurtzoid2c and 1.70 a.u at 761 cm<sup>-1</sup> for triwurtzoid). Therefore, we can say that the intensity of IR

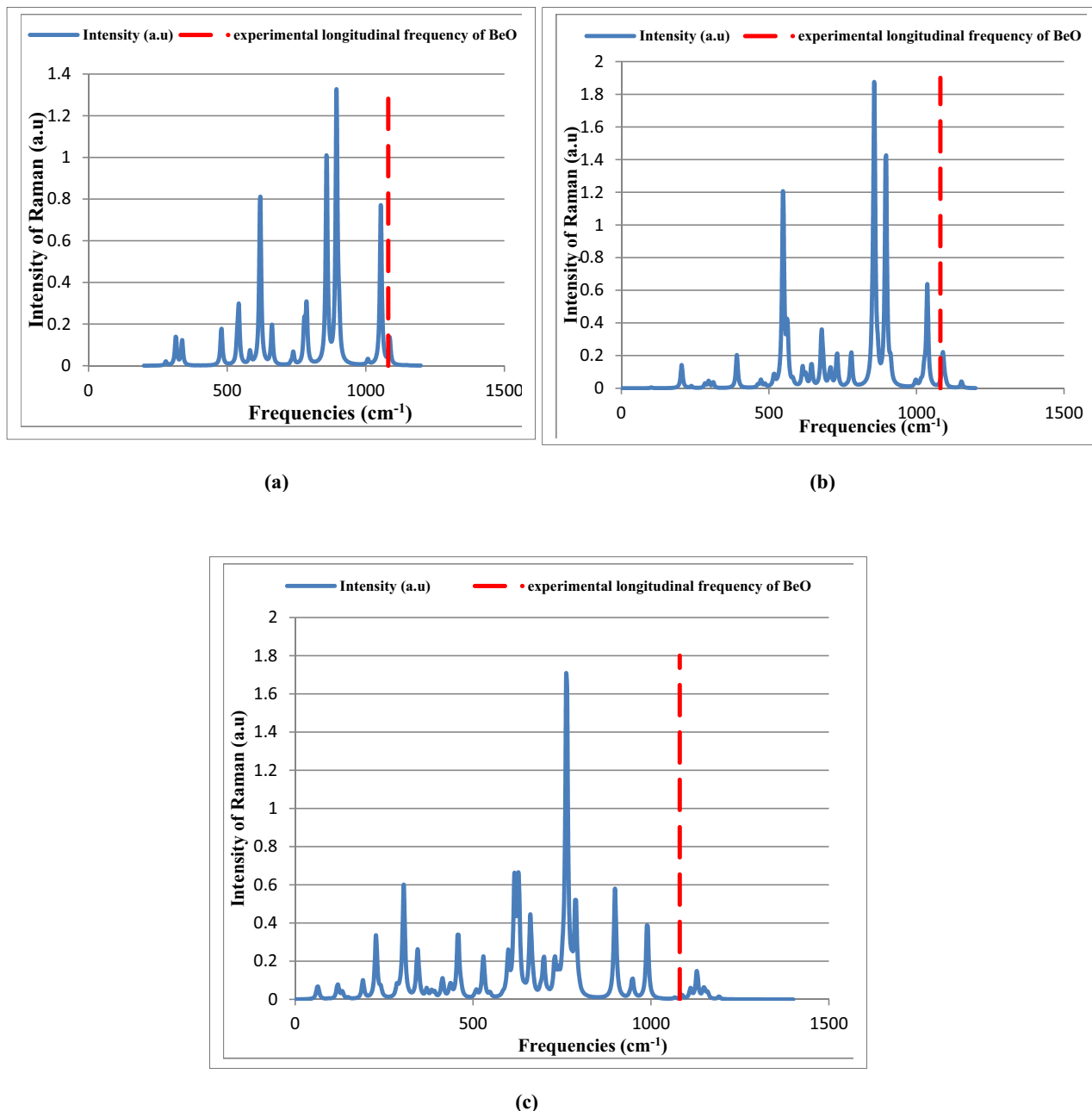


**Fig. 6.** (a) The intensity of Raman of wurtzoid Be<sub>7</sub>O<sub>7</sub>, (b) The intensity of Raman of wurtzoid2c Be<sub>13</sub>O<sub>13</sub>, (c) The intensity of Raman of triwurtzoid Be<sub>21</sub>O<sub>21</sub>, compare with the experimental longitudinal frequency of BeO bulk.

increases with increase size at nanoscale . The theoretical and experimental values of longitudinal frequency (LO) of BeO bulk is (1127.1 cm<sup>-1</sup>) [28] and (1081 cm<sup>-1</sup>) [9], respectively.

### 3.2.2. Reduced mass and force constant

Fig. 7(a,b and c) shows the reduced masses of the BeO at nanoscale limited (wurtzoid, wurtzoid2c and triwurtzoid), respectively, as a function of frequencies, and Fig. 8(a,b and c) shows the force

constant of the BeO at nanoscale limited (wurtzoid, wurtzoid2c and triwurtzoid) respectively, as a function of frequencies.

$$v = \frac{1}{2\pi} \sqrt{\frac{k}{\mu}}$$

where k and μ are force constant and reduced mass of molecules. The frequencies were proportioned with force constant but inversely with the reduced mass, and the value of both of them in this paper corresponds with highest value of LO mode. The force con-

stant represents the parabola shape as a function of frequencies as shown in eq (1) [29].

The longitudinal mode frequencies (LO) represent the last point in reducing mass and its value around (1102, 1106 and

1151  $\text{cm}^{-1}$ ), which is agreed with the theoretical and experimental values of (LO) for BeO bulk (1127.1  $\text{cm}^{-1}$ ) [28] and (1081  $\text{cm}^{-1}$ ) [9], respectively.

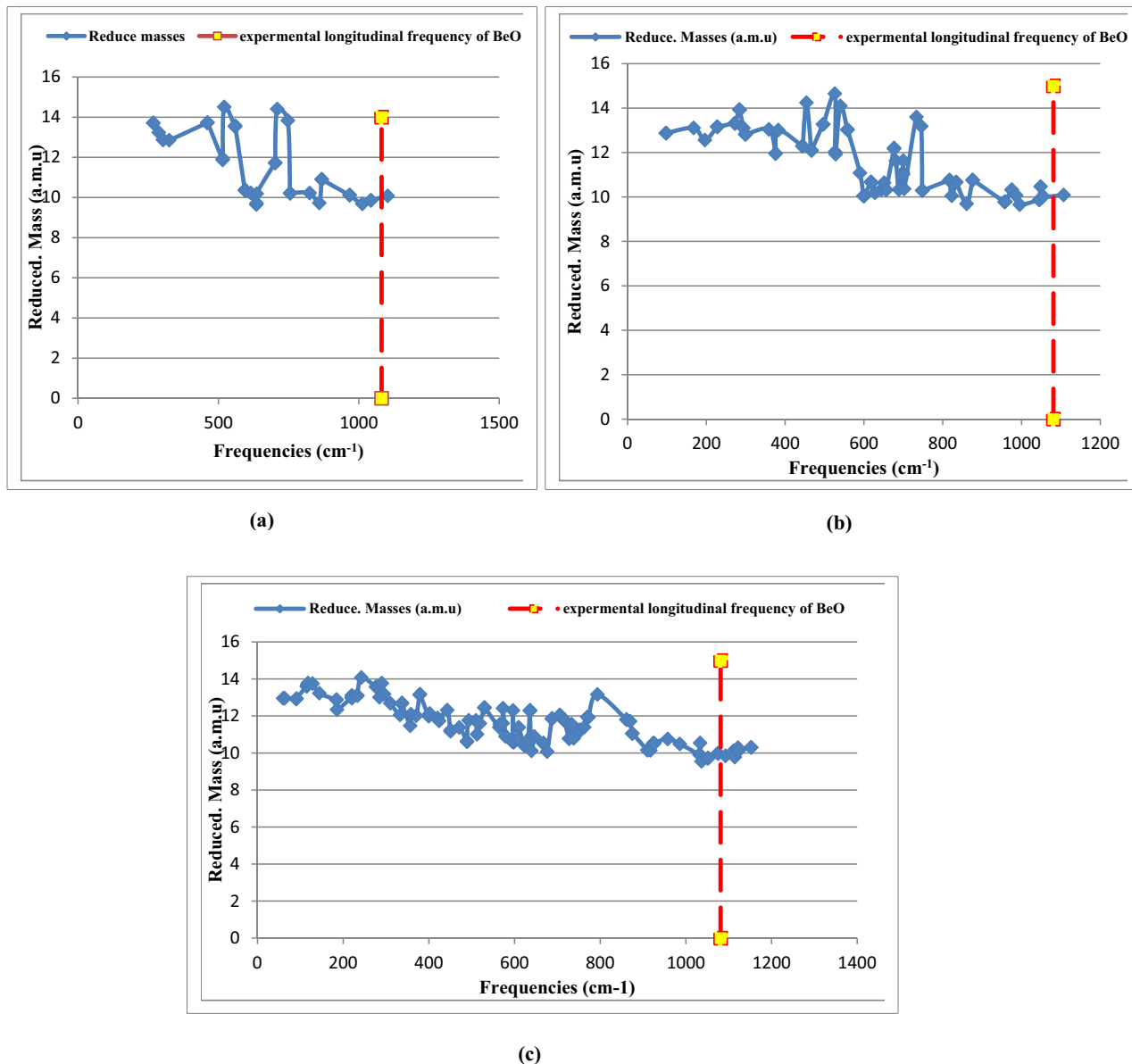


Fig. 7. (a) The reduced mass as a function of the frequency of wurtzoid  $\text{Be}_7\text{O}_7$ , (b) The reduced mass as a function of the frequency of wurtzoid2c  $\text{Be}_{13}\text{O}_{13}$ , (c) The reduced mass as a function of the frequency of triwurtzoid  $\text{Be}_{21}\text{O}_{21}$ , compare with the experimental LO vibrational mode of BeO.

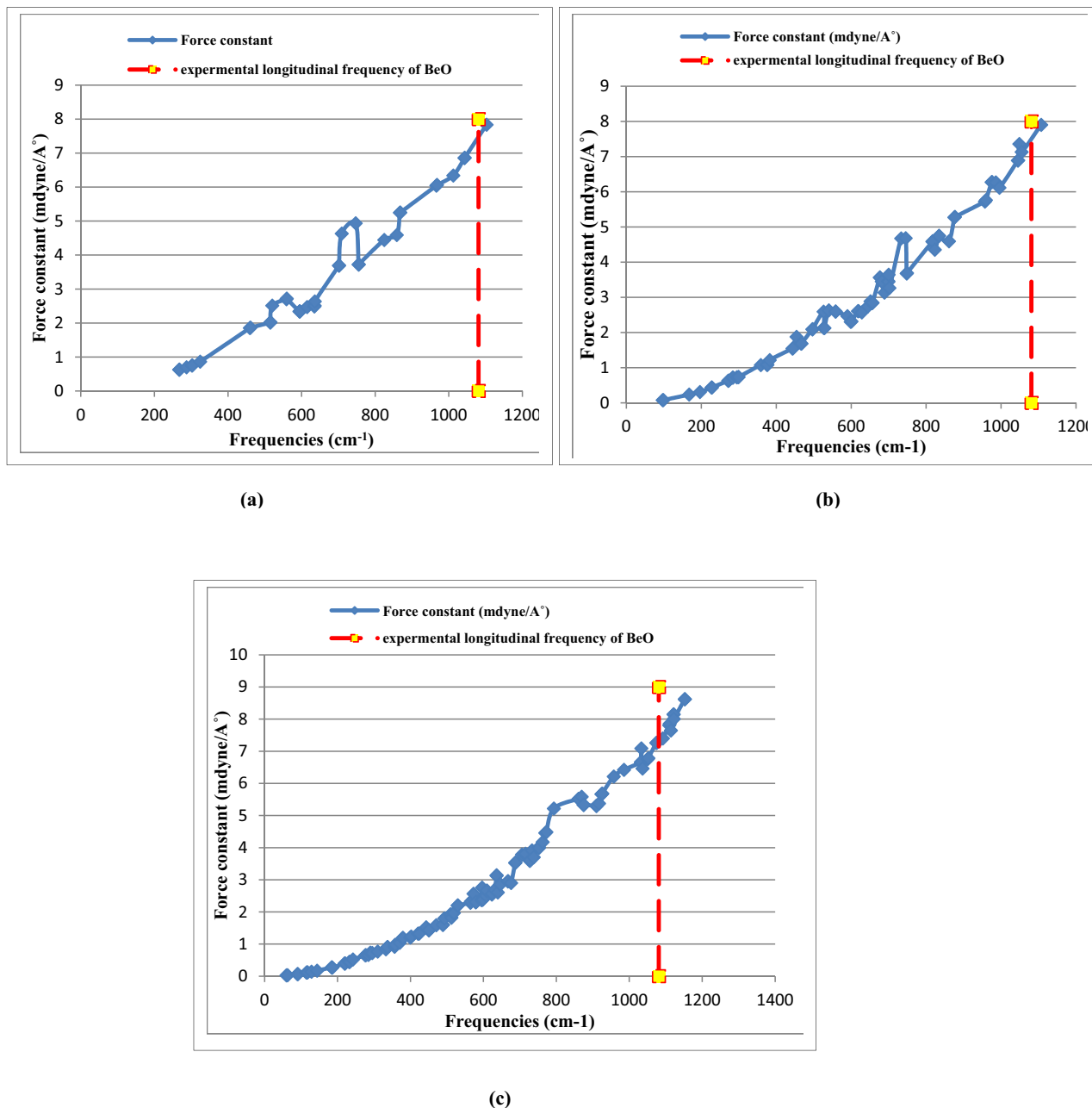


Fig. 8. (a) The force constant as a function of the frequency of wurtzoid Be<sub>7</sub>O<sub>7</sub>, (b) The force constant as a function of the frequency of wurtzoid2c Be<sub>13</sub>O<sub>13</sub>, (c) The force constant as a function of the frequency of triwurtzoid Be<sub>21</sub>O<sub>21</sub>, compare with the experimental LO vibrational mode of BeO.

#### 4. Conclusion

In the current work, we have nanotubes were investigated theoretically to calculate electronic and spectroscopic properties of BeO wurtzoid by using basis set of B3LYP-6-31G\* and employed the approximation methods (GGA) of the Density Functional Theory. The obtained results can be summarized as follows:

**a-** The energy gap depends on size, shape and surface conditions, and it found that the energy gap increases when we increase the size of BeO wurtzoids, because the effect of the surface dangling bonds.

**b-** The density of state of BeO wurtzoids structure increases with increasing of size.

**c-** The bond lengths have distribution in which the highest peaks are close and agreed with bulk values.

**d-** It can be noticed that the geometry of structures as wurtzoid and wurtzoid-2c as two tubes sharing along c - constant while triwurtzoid (three tubes) which form a capped bundle (3,0) nanotube.

**e-** The longitudinal optical mode of BeO wurtzoid is agreed with the experimental longitudinal optical of BeO bulk.

#### Declaration of Competing Interest

The authors declare that they have no known competing financial interests or personal relationships that could have appeared to influence the work reported in this paper.

#### References

[1] P.E. Van Camp, V.E. Van Doren, Ground-state properties and structural phase transformation of beryllium oxide, *J. Phys. Condens. Matter* 8 (19) (1996) 3385.



- [2] A. Continenza, R.M. Wentzcovitch, A.J. Freeman, Theoretical investigation of graphitic BeO, *Phys. Rev. B* 41 (6) (1990) 3540.
- [3] V.A. Sashin, M.A. Bolorizadeh, A.S. Kheifets, M.J. Ford, Electronic band structure of beryllium oxide, *J. Phys. Condens. Matter* 15 (21) (2003) 3567.
- [4] D.W. Rankin, D.R. Lide. "Crystallography reviews." CRC handbook of chemistry and physics 15 (2009): P.223-4.
- [5] V.S. Kiiko, A.V. Pavlov, V.A. Bykov. "Production and thermophysical properties of BeO ceramics with the addition of nanocrystalline titanium dioxide." *Refract. Ind. Ceram.* 59, no. 6 (2019): PP.616-622.
- [6] D. Koh, J.-H. Yum, S.K. Banerjee, T.W. Hudnall, C. Bielawski, W.A. Lanford, B.L. French, et al., Investigation of atomic layer deposited beryllium oxide material properties for high-k dielectric applications, *J. Vacuum Sci. Technol. B Nanotechnol. Microelectron. Mater. Process. Measure. Phenomena* 32 (3) (2014) 03D117.
- [7] G.P. Akishin, S.K. Turnaev, V. Ya Vaispapor, M.A. Gorbunova, Yu N. Makurin, V.S. Kiiko, A.L. Ivanovskii. "Thermal conductivity of beryllium oxide ceramic." *Refract. Ind. Cerami.* 50, no. 6 (2009): PP.465-468.
- [8] S. Duman, A. Sütlü, S. Bağcı, H.M. Tütüncü, G. . Srivastava. "Structural, elastic, electronic, and phonon properties of zinc-blende and wurtzite BeO." *J. Appl. Phys.* 105, no. 3 (2009):P. 033719.
- [9] A. Bosak, K. Schmalzl, M. Krisch, W. van Beek, V. Kolobanov. "Lattice dynamics of beryllium oxide: Inelastic x-ray scattering and ab initio calculations." *Phys. Rev. B* 77, no. 22 (2008):P. 224303.
- [10] W. Zhu, J.P. Han, T.P. Ma. "Mobility measurement and degradation mechanisms of MOSFETs made with ultrathin high-k dielectrics." *IEEE Trans. Electron Devices* 51, no. 1 (2004): PP.98-105.
- [11] C.W Peterson, G.E. Palma. "BeO as a window in the vacuum uv." *JOSA* 63, no. 3 (1973): PP.387-388.
- [12] M.A. Abdulsattar. "Caped ZnO (3, 0) nanotubes as building blocks of bare and H passivated wurtzite ZnO nanocrystals." *Superlattices Microstruct.* 85 (2015): PP.813-819.
- [13] M.T. Hussein, M.A. Abdulsattar, H.A. Hameed, Electronic and vibrational spectroscopic properties of GaAs diamondoids using Density Functional Theory, *Int. J. Adv. Ind. Eng.* 2 (4) (2014) 150–156.
- [14] M.A. Abdulsattar, M.T. Hussein, T.H. Mahmood, Stability, electronic and vibrational properties of GaIn wurtzoid molecules and nanocrystals: A DFT study, *Vacuum* 153 (2018) 17–23.
- [15] M.T. Hussain, H.A. Thjeel. "Study of Geometrical and Electronic properties of ZnS wurtzoids via DFT." *Chalcogenide letters* 15, no. 10 (2018): PP.523-528.
- [16] M.T. Hussein, H.A. Thjeel, February. Vibration Properties of ZnS nanostructure Wurtzoids: ADFT Study. In *Journal of Physics: Conference Series* (Vol. 1178, No. 1, 2019, p. 012015). IOP Publishing.
- [17] M.A. Abdulsattar, M.T. Hussein, T.A. Fayad, Composition effects on formation energies, electronic and vibrational properties of ZnCdS wurtzoid molecules: A DFT study, *Optik* 202 (2020) 163674.
- [18] M.T. Hussein, T.A. Fayad, M.A. Abdulsattar, "concentration effects on electronic and spectroscopic properties of ZnCds wurtzoids: A density functional theory study" *Chalcogenide Lett.* vol.16,No.11,November 2019,PP.557-563.(Thomson Reuters).
- [19] M.T. Hussein, A. Ramizy, B.K. Ahmed. "First principles calculations of Al AsxP1-x ternarynanocrystalalloying composition." *Iraqi J. Phys.* 15, no. 33 (2017): PP.54-62.
- [20] M.J. Van Setten, R. Gremaud, G. Brocks, B. Dam, G. Kresse, G.A. De Wijs, Optical response of the sodium alanate system: GW 0-BSE calculations and thin film measurements, *Phys. Rev. B* 83 (3) (2011) 035422.
- [21] NIST Computational Chemistry Comparison and Benchmark Database NIST Standard Reference Database Number 101 Release 18, October 2016, Editor: Russell D. Johnson III [Accessed: 29-Jan-2017].
- [22] M.J. Frisch, G.W. Trucks, H.B. Schlegel, G.E. Suzerain, M.A. Robb, J.R. Cheeseman, J.A. Montgomery, Jr., T. Vreven, K.N. Kudin, J.C. Burant, J.M. . Millam, S.S. Iyengar, J. Tomasi, V. Barone, B. Mennucci, M. Cossi, G. Scalmani, N. Rega, G.A. Petersson, H. Nakatsuji, M. Hada, M. Ehara, K. Toyota, R. Fukuda, J. Hasegawa, M. Ishida, T. Nakajima, Y. Honda, O. Kitao, H. Nakai, M. Klene X. Li, J. E. Knox, H.P. Hratchian, J.B. Cross, C. Adamo, J. Jaramillo, R. Gomperts, R. E. Stratmann, O. Yazyev, A. J. Austin, R. Cammi, C. Pomelli, J.W. Ochterski, P.Y. Ayala, K. Morokuma, G.A. Voth, P. Salvador, J.J. Dannenberg, V. G. Zakrzewski, S. Dapprich, A.D. Daniels, M.C. Strain, O. Farkas, D.K. Malick, A.D. Rabuck, K. Raghavachari, J.B. Foresman, J.V. Ortiz, Q. Cui, A.G. Baboul, S. Clifford, J. Cioslowski, B.B. Stefanov, G. Liu, A. Liashenko, P. Piskorz, I. Komaromi, R.L. Martin, D.J. Fox, T. Keith, M.A. Al-Laham, C.Y. Peng, A. Nanayakkara, M. Challacombe, P.M.W. Gill, B. Johnson, W. Chen, M.W. Wong, C. Gonzalez, J.A. Pople, Gaussian, Inc., Pittsburgh PA, (2003).
- [23] H. Ünlü, "A thermodynamic model for determining pressure and temperature effects on the band gap energies and other properties of some semiconductors." *Solid-State Electron.* 35, no. 9 (1992): PP.1343-1352.
- [24] B. Amrani, F El Haj. Hassan, H. Akbarzadeh. "First-principles investigations of the ground-state and excited-state properties of BeO polymorphs." *J. Phys. Condens. Matter* 19, no. 43 (2007): P.436216.
- [25] Y. Rostamiyan, V. Mohammadi, Amin Hamed Mashhadzadeh, Mechanical, electronic and stability properties of multi-walled beryllium oxide nanotubes and nanopeapods: A density functional theory study, *J. Mol. Model.* 26 (4) (2020) 1–13.
- [26] J. Beheshtian, I. Ravaei. "Hydrogen storage by BeO nano-cage: A DFT study." *Appl. Surface Sci.* 368 (2016): PP.76-81.
- [27] Y-G. Chen, M. Xing, Y. Guo, Z. Lin, X. Fan, X.-Ming Zhang. "BeO6 Trigonal prism with ultralong Be–O Bonds observed in a deep ultraviolet optical crystal Li13Be6B9O27." *Inorgan. Chem.* 58, no. 3 (2019): P.2201-2207.
- [28] U.D. Wdowik, "Structural stability and thermal properties of BeO from the quasiharmonic approximation." *J. Phys. Condens. Matter* 22, no. 4 (2010):p. 045404.
- [29] C. Kittel, "Introduction to solid state physics, eight editions, library of congress cataloging." (2005).